



OPEN ACCESS

EDITED BY

Qing Luo,
Shenyang University, China

REVIEWED BY

Chao Wang,
Guangdong Ocean University, China
Qinghui Huang,
Tongji University, China

*CORRESPONDENCE

Rongguo Su
✉ surongguo@ouc.edu.cn
Ying Bai
✉ baiying@ysfri.ac.cn

SPECIALTY SECTION

This article was submitted to
Marine Pollution,
a section of the journal
Frontiers in Marine Science

RECEIVED 27 December 2022

ACCEPTED 14 February 2023

PUBLISHED 01 March 2023

CITATION

Liu S, Cui Z, Bai Y, Ding D, Yin J, Su R and
Qu K (2023) Indirect photodegradation of
ofloxacin in simulated seawater: Important
roles of DOM and environmental factors.
Front. Mar. Sci. 10:1132216.
doi: 10.3389/fmars.2023.1132216

COPYRIGHT

© 2023 Liu, Cui, Bai, Ding, Yin, Su and Qu.
This is an open-access article distributed
under the terms of the [Creative Commons
Attribution License \(CC BY\)](https://creativecommons.org/licenses/by/4.0/). The use,
distribution or reproduction in other
forums is permitted, provided the original
author(s) and the copyright owner(s) are
credited and that the original publication in
this journal is cited, in accordance with
accepted academic practice. No use,
distribution or reproduction is permitted
which does not comply with these terms.

Indirect photodegradation of ofloxacin in simulated seawater: Important roles of DOM and environmental factors

Shukai Liu^{1,2}, Zhengguo Cui², Ying Bai^{2*}, Dongsheng Ding²,
Junshuang Yin², Rongguo Su^{1*} and Keming Qu²

¹Laboratory of Marine Chemistry Theory and Technology, Ministry of Education, Ocean University of China, Qingdao, China, ²Key Laboratory of Sustainable Development of Marine Fisheries, Ministry of Agriculture and Rural Affairs, Laboratory for Marine Fisheries Science and Food Production Processes, Yellow Sea Fisheries Research Institute, Chinese Academy of Fishery Sciences, Qingdao, China

Dissolved organic matter (DOM) plays a non-negligible role in the indirect photodegradation of organic contaminants. This research investigated the roles of DOM and the environmental factors (salinity, pH, NO₃⁻, and HCO₃⁻) in the indirect photodegradation of ofloxacin (OFX) in simulated seawater. Results showed that DOM can significantly accelerate the indirect photodegradation of OFX, and ¹O₂ and ³DOM* were the main reactive intermediates (RIs) that could promote the indirect photodegradation of OFX. Fluorescence excitation–emission matrix spectroscopy–parallel factor analysis (EEMs-PARAFAC) was used to divide DOM into four fluorescence components. The indirect photodegradation rate of OFX was affected by DOM structure, and terrigenous DOM usually produced more RIs to promote the indirect photodegradation of OFX. Increased salinity significantly promotes the indirect photodegradation of OFX, while increased NO₃⁻ concentration had no effect on the OFX indirect photodegradation. pH affected the formation of RIs and the structure of OFX, thereby affecting the indirect photodegradation of OFX. The indirect photodegradation rate of OFX increased in the HCO₃⁻ solution, which is due to the formation of carbonate radical (CO₃⁻). This study is essential in understanding the role of DOM in OFX indirect photodegradation and providing a novel insight into the fate, removal, and transformation of OFX.

KEYWORDS

dissolved organic matter, ofloxacin, indirect photodegradation, DOM components, environmental factors

1 Introduction

Pharmaceuticals and personal care products (PPCPs) are considered new organic pollutants, including various antibiotics, biopharmaceuticals, and fungicides, which have raised scientific and public concern over the past decades. PPCPs are usually detected in drinking water, sewage, and wastewater treatment plants (WWTPs) due to their universal

consumption, diversity, and unique chemical properties (Yang et al., 2017). Generally, most antibiotics and their metabolites ingested by humans and animals are excreted with urine and feces and subsequently spread to the environment. The concentrations of sulfonamides, fluoroquinolones (FQs), and macrolide compounds in wastewater from animal production and pharmaceutical companies are as high as 200, 98, and 5.6 mg L⁻¹, respectively (Zhang et al., 2021). It has been demonstrated that antibiotic residues in the environment can lead to the evolution of new drug-resistant bacteria and increase bacterial resistance, which ultimately pose threats to aquatic ecosystems and human health. FQs are a family of synthetic antimicrobial agents for both humans and animals, which have been detected at high concentrations in aquatic environments in Europe, America, Australia, and Asia (Al Aukidy et al., 2012). Ofloxacin (OFX), one of the FQs, can be detected in a variety of natural water and even in drinking water and groundwater. It has been detected at a maximum of tens of µg L⁻¹ in WWTPs and at hundreds of ng L⁻¹ in surface water (Danner et al., 2019; Ding et al., 2020). Due to animal husbandry and aquaculture having produced a large amount of industrial and aquacultural waste, notable antibiotic residues were transported to coastal areas through riverine inputs and precipitation (Fu et al., 2003; Zhang et al., 2013). The ocean has become an important sink of many antibiotics. Hence, it is important to understand the behavior of OFX in seawater for its environmental risk assessment.

The removal of OFX from aquatic environments has been extensively researched, such as physical, chemical, and biological methods (Tian et al., 2021). Generally, photodegradation is considered the main degradation pathway of OFX in natural water. It is well known that direct photodegradation involves energy and electron transfer after dissolved organic matter (DOM) absorbs photons (Du et al., 2014). Indirect photodegradation refers to the process in which some photosensitizers generate reactive intermediates (RIs) to degrade organic contaminants (Yang et al., 2013). DOM is a diverse and complex mixture that acts as a photosensitizer in the natural environment. Generally, the photodegradation of DOM results in the formation of RIs, such as hydroxyl radical ($\cdot\text{OH}$), singlet oxygen ($^1\text{O}_2$), and the reactive triplet state(s) of DOM ($^3\text{DOM}^*$), which can facilitate the indirect photodegradation of OFX (Burns et al., 2012). However, DOM can also restrain the photodegradation process through light attenuation, quenching RIs, and back-reduction mechanisms (Wu et al., 2021). Numerous studies have demonstrated that the ability of DOM to generate RIs was dependent on the source of DOM and the content of functional groups, resulting in different effects on the photodegradation of organic pollutants (Guerard et al., 2009; Liu et al., 2021). For example, DOM from soil usually has high aromaticity and degree of humification (Xu et al., 2018), which can produce high concentrations of RIs to promote the photodegradation of organic pollutants. In contrast, DOM extracted from seawater contains lower aromatic C=C and C=O functional groups and exhibits lower steady-state concentrations of RIs compared with freshwater DOM, thus having less effect on the photodegradation of organic pollutants (Wang et al., 2019). Therefore, it is necessary to explore the effect of DOM components on the indirect

photodegradation of OFX. Excitation–emission matrix spectroscopy (EEMs) can distinguish different classes of materials of terrestrial, autogenous, and anthropogenic origin by concatenating continuous emission spectra of a range of excitation wavelengths (Coble et al., 1998). The technique of EEMs combined with parallel factor analysis (PARAFAC) has been used for evaluating the composition, origin, and fate of DOM (Guéguen et al., 2011). Moreover, ultraviolet–visible spectroscopy (UV–Vis) technology can be used to reflect the degree of humification and aromaticity of DOM. Therefore, we used EEMs-PARAFAC and UV–Vis to study the relationship between DOM components and OFX indirect photodegradation.

Other environmental factors in seawater also can affect the generation of RIs, thus having an impact on the photodegradation of organic pollutants. It has been demonstrated that NO_3^- , HCO_3^- , salinity, and pH are crucial factors in seawater to influence the indirect photodegradation of organic pollutants (Bai et al., 2018; Wang et al., 2021). NO_3^- can produce $\cdot\text{OH}$ through direct photolysis under solar radiation to affect the photodegradation of organic pollutants, and the quantum yield of $\cdot\text{OH}$ was affected by pH (Bodrato and Vione, 2014). In natural water, HCO_3^- can react with $\cdot\text{OH}$ to influence the formation of CO_3^- , which is a selective oxidant and plays an important role in aquatic oxidation reactions. The reaction between CO_3^- and organic pollutants mainly occurs through electron transfer or hydrogen extraction mechanism (Liu et al., 2018). Additionally, pH and salinity can affect the indirect photodegradation of organic pollutants by affecting the generation of RIs or the structure of organic pollutants.

Previous studies have reported that the indirect photodegradation of OFX in freshwater accounted for more than 50% of the observed photodegradation rate (Cheng et al., 2021). Lam and Mabury (2005) reported that the photosensitive reaction or photooxidant produced by DOM photolysis played a great role in the photodegradation of OFX in synthetic field water. However, the effect of DOM components on the indirect photodegradation of OFX is still unknown, and there are no data available on the indirect photodegradation of OFX in seawater. It limited the research about the mechanism of photodegradation of organic pollutants. In this study, we investigated the indirect photodegradation of OFX and environmental factors in simulated seawater, especially the roles of DOM in simulated seawater on the indirect photodegradation of OFX. This study aims to 1) explore the roles of DOM and RIs ($^1\text{O}_2$, $\cdot\text{OH}$, and $^3\text{DOM}^*$) in the indirect photodegradation of OFX, 2) investigate the effects of DOM components on the indirect photodegradation of OFX, and 3) study the effect of other environmental factors (pH, salinity, NO_3^- , and HCO_3^-) in DOM solutions on the indirect photodegradation of OFX. It provides an important theoretical basis for the scientific assessment of the fate and environmental risk of OFX.

2 Materials and methods

2.1 Materials

OFX ($\geq 99\%$), isopropanol (IPA; $\geq 99.9\%$), furfuryl alcohol (FFA, $\geq 98\%$), and sorbic acid (SA; $\geq 99.0\%$) were obtained from Sigma-

Aldrich (, St. Louis, MO, USA). 2-Hydroxyterephthalic acid (2OHTA) was synthesized. Tetrahydrofuran (THF) was acquired from Tianjin Fuyu Fine Chemical Co., Ltd. (Tianjin, China). Suwannee River humic acid (SRHA, 3S101H) and Suwannee River fulvic acid (SRFA, 3S101F) were obtained from the International Humic Substances Society (Denver, CO, USA). Another humic acid (JKHA) was acquired from J&K Scientific Ltd. (Beijing, China). Other inorganic solvents (NaNO₃, NaHCO₃, NaOH, and HCl) and indole were purchased from Sinopharm Chemical Reagent Beijing Co., Ltd. (Beijing, China). Acetonitrile and methanol (high-performance liquid chromatography (HPLC) grade) were obtained from Merck (Darmstadt, Germany). International Association for the Physical Sciences of the Ocean (IAPSO) standard seawater was purchased from Ocean Scientific International Ltd. (Havant, UK). The concentrations of DOM stock solutions were set to 2, 5, and 10 mg C L⁻¹ at pH 8.0 ± 0.1. The concentration of dissolved organic carbon (DOC) is calculated by the formula [DOC] = M_{DOM} × C%, where M_{DOM} is the quality of DOM and C% is the carbon content percentage. The carbon content percentages of SRFA, SRHA, and JKHA are 52.34%, 52.63%, and 40.0%, respectively. All solutions were prepared using ultrapure water (18.2 MΩ cm⁻¹, Milli-Q, Millipore, Billerica, MA, USA).

2.2 Photochemical experiments

The XPA-7 merry-go-round photoreactor (Xujiang Electromechanical Plant, Nanjing, China) is equipped with a 1,000-W xenon arc lamp to perform photochemical experiments. The filter film was wrapped around the lamp to decrease the irradiation below 320 nm to reduce the direct photodegradation of OFX. To eliminate the influence of thermal and hydrolysis processes, the degradation rate of OFX was determined under dark conditions. The OFX initial concentration was 10 μM, and the pH of the OFX stock solution was controlled to 8.0 ± 0.1. The light intensity was maintained at 200 W m⁻² from 320 nm to 800 nm, and the temperature was maintained at 25°C ± 1°C. The configured DOM solutions were irradiated in a photochemical reactor for 24 h, and then the concentration of OFX was determined.

FFA (20 mM) and IPA (10 mM) were added to OFX solutions containing JKHA to scavenge ¹O₂ and ·OH in ultrapure water to explore the self-sensitization of OFX. IPA (10 mM), indole (5 mM), THF (10 mM), and SA (20 mM) were used to scavenge ·OH, ¹O₂, CO₃⁻, and ³DOM*, respectively. The JKHA solutions with different salinity were obtained by diluting IAPSO standard seawater to explore the effect of salinity on the indirect photodegradation of OFX. The dilute solutions of NaOH and HCl were used to adjust the pH to experimental values (5.0, 7.0, 9.0, 11.0), and different concentrations of nitrate (0–40 μM) and bicarbonate (2 mM) were prepared in JKHA solutions to explore the impacts of some common ions on the indirect photodegradation of OFX. During irradiation, a 2-ml sample solution was taken regularly and transferred to an amber liquid phase vial.

The light screening factor (S_λ) and total light screening coefficient (f) were used to correct the light screening effects (Eqs

1, 2).

$$S_{\lambda} = \frac{1 - (10^{-(\alpha_{\lambda} + \varepsilon_{\lambda}[\text{OFX}]l)})}{2.303(\alpha_{\lambda} + \varepsilon_{\lambda}[\text{OFX}]l)}, \quad (1)$$

$$f = \frac{\sum I_{\lambda} S_{\lambda} \varepsilon_{\lambda}}{\sum I_{\lambda} \varepsilon_{\lambda}}, \quad (2)$$

where α_λ is the light attenuation coefficient (cm⁻¹), α_λ = 2.303A/l, A is the absorbance, ε_λ is the molar absorptivity (L mol⁻¹ cm⁻¹), l is the light path length (cm), and [OFX] is the concentration of OFX (mol L⁻¹). The indirect photodegradation rate of OFX is calculated as follows:

$$k_{\text{ind}} = k_{\text{obs(DOM)}} - k_{\text{obs(non-DOM)}} * f, \quad (3)$$

where k_{obs(DOM)} represents the observed photodegradation rate of OFX with the addition of DOM, k_{obs(non-DOM)} is the observed photodegradation rate in ultrapure water, and k_{ind} is the corrected indirect photodegradation rate of OFX.

2.3 Determination of RI content

RIs are commonly analyzed with probe components (PCs) in aquatic environments. FFA was used as a PC to detect the concentration of ¹O₂. SA was used as a quantitative probe to determine the steady-state concentration of ³DOM*. Terephthalic acid (TA) was used to determine the concentration of ·OH.

The concentration of ³DOM* was measured by determining the concentration of SA. The removal rate of ³DOM* by SA was obtained by dividing the rate of SA *cis-trans* isomer formation by 0.18, which is the yield of SA. The concentration of PC is divided by the rate constant of sorbic acid, and the probe concentration was plotted according to Eq. (4).

$$\frac{[\text{SA}]}{[\text{R}_{\text{SA}}]} = \frac{[\text{SA}]}{R_{3_{\text{DOM}^*}}} + \frac{k'_s}{R_{3_{\text{DOM}^*}} k_{\text{SA},3_{\text{DOM}^*}}}, \quad (4)$$

where R_{3_{DOM}*} represents the formation rate of ³DOM*, k'_s is the reaction rate constants of quenchers with the triplets, and k_{SA,3_{DOM}*} is the reaction rate between SA and ³DOM*, which Timko et al. (2014) have already calculated as (3.35 ± 1.0) × 10⁹ M⁻¹ S⁻¹. Formation rates of triplets were calculated as the inverse of the slope, while k'_s and steady-state concentrations of ³DOM* ([³DOM*]_{ss}) (in the absence of probe) were determined as follows:

$$k'_s = k_{\text{SA},3_{\text{DOM}^*}} \cdot \frac{\text{intercept}}{\text{slope}}, \quad (5)$$

$$[{}^3\text{DOM}^*]_{\text{ss}} = \frac{R_{3_{\text{DOM}^*}}}{k'_s} \quad (6)$$

The steady-state concentration of ·OH in DOM solutions was determined through the addition of TA (600 μM). The concentration of ·OH can be obtained by measuring the concentration of HOTA (Eqs 7, 8). Samples were taken at different time periods, and the concentration of HOTA was

determined by HPLC.



$$k_{\text{obs}} = \gamma \times k_{\text{OH,TA}}[\cdot\text{OH}]_{\text{ss}}, \quad (8)$$

where $k_{\text{OH,TA}} = 3.3 \times 10^9 \text{ M}^{-1} \text{ s}^{-1}$ and γ is the yield of HOTA, which is 0.35.

FFA was routinely used as the PC of $^1\text{O}_2$ in determining the concentration of $^1\text{O}_2$. The DOM solution containing FFA (20 mM) was irradiated, and the steady-state concentration of $^1\text{O}_2$ was determined by measuring the concentration of FFA (Eqs 9, 10).



$$\frac{d[\text{FFA}]}{dt} = -k_{1\text{O}_2,\text{FFA}}[\text{FFA}][^1\text{O}_2]_{\text{ss}}, \quad (10)$$

where $k_{1\text{O}_2,\text{FFA}} = 1.2 \times 10^8 \text{ M}^{-1} \text{ s}^{-1}$, and $[^1\text{O}_2]_{\text{ss}}$ is the steady-state concentration of $^1\text{O}_2$. Samples were taken regularly, and all solutions were measured by HPLC.

2.4 Analytical method

The concentration of OFX was determined by an HPLC instrument (1100 series, Agilent Technologies, Santa Clara, CA, USA) equipped with UV-visible and fluorescence detectors and Agilent PLRP-S C18 column (4.6 × 150 mm, 4 μM). The flow rate, detection wavelength, mobile phase, and injection volume are shown in Table S1.

The EEMs of DOM were measured using a fluorescence spectrophotometer (Fluorolog3-11) equipped with a 450-W xenon arc lamp. The excitation wavelength of EEMs was from 240 to 480 nm, the emission wavelength was 250–580 nm, the interval of excitation and emission wavelengths was 5 nm, the integration time was 0.05 s, and the scanning speed was 1,200 nm min⁻¹. The slit width of excitation and emission was 5 nm. Before detection, the samples were all filtered through a 0.22-μm polyether sulfone membrane. The 3D Delaunay interpolation method was used to eliminate the scattering peaks of the fluorescence spectrum. The fluorescence spectrum was calibrated against the quinine sulfate standard, and the data were normalized to the unit of quinine sulfate (QSU).

The humification index (HIX) was obtained by dividing the emission intensity at 435–480 nm by the integral intensity at 300–345 nm at an excitation wavelength of 255 nm, and it was used to characterize the humification degree and source of DOM (Ohno and Technology, 2002). Specific UV absorbance (SUVA₂₅₄) was defined as the UV absorbance at 254 nm divided by the DOC concentration, which strongly correlated with DOM aromaticity (Weishaar et al., 2003). All data were measured by fluorescence spectrophotometer and analyzed by PARAFAC in MATLAB R2012a software.

SPSS 26.0 and Canoco 5.0 were used to analyze the correlation of the k_{ind} , DOM components, HIX, SUVA₂₅₄, and the concentrations of RIs. The indirect photodegradation experiments

of OFX were performed in parallel three times, and the error was controlled within 5%.

3 Results and discussion

3.1 Direct photodegradation of OFX

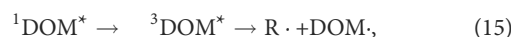
We found no loss of OFX concentration under dark conditions for 24 h, indicating that hydrolysis and biodegradation played negligible roles in the degradation of OFX. The photodegradation rate of OFX in ultrapure water followed pseudo-first-order kinetics, and OFX was degraded by approximately 27.7% after 24 h under simulated sunlight irradiation at pH 8.0 (Figure S1A). We found that there was an absorption of OFX between 320 and 400 nm (Figure S1B), indicating that the direct photodegradation of OFX was not completely deducted. Therefore, we used f to correct the indirect photodegradation of OFX.

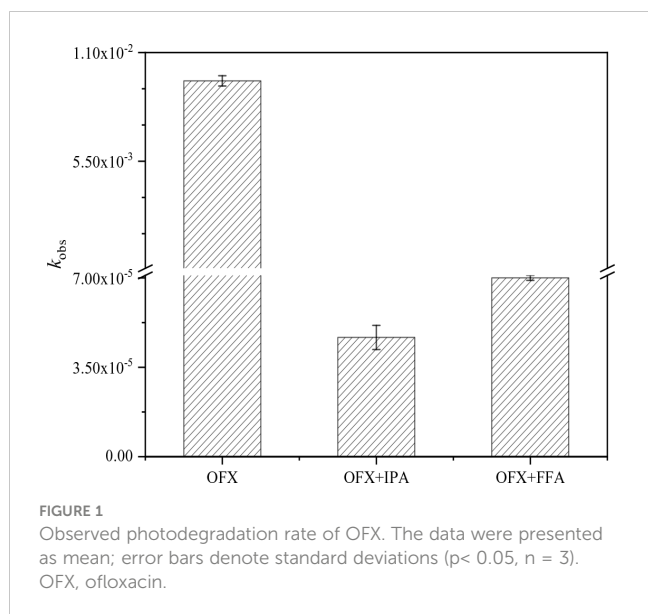
Niu et al. (2016) presented that the photodegradation process mediated by triplet states of pollutants and their induced reactive oxygen species was considered self-sensitized photodegradation. Previous studies demonstrated that $\cdot\text{OH}$ and $^1\text{O}_2$ might play important roles in the self-sensitized photolysis of acetotolol (Ge et al., 2010; Ye et al., 2022). Zhu et al. (2014) reported that phenylarsonic compounds were mainly photodegraded by self-sensitization, starting with the formation of the excited triplet-state molecules. In our study, quenching experiments were performed to explore whether $\cdot\text{OH}$ and $^1\text{O}_2$ affect the self-sensitized photodegradation of OFX, for which the results are shown in Figure 1. The addition of IPA/FFA significantly inhibited the photodegradation of OFX. These results meant that the self-sensitized photodegradation of OFX might be conducted through $\cdot\text{OH}$ and $^1\text{O}_2$.

3.2 Roles of DOM in the OFX indirect photodegradation

3.2.1 Roles of DOM

DOM was the main form of organic matter in the aquatic environment, and it can combine with metals and organic pollutants, affecting the distribution and fate of organic pollutants. Meanwhile, photolysis of DOM can produce RIs to promote the indirect photodegradation of organic pollutants (Eqs 11–17) (Burns et al., 2012).





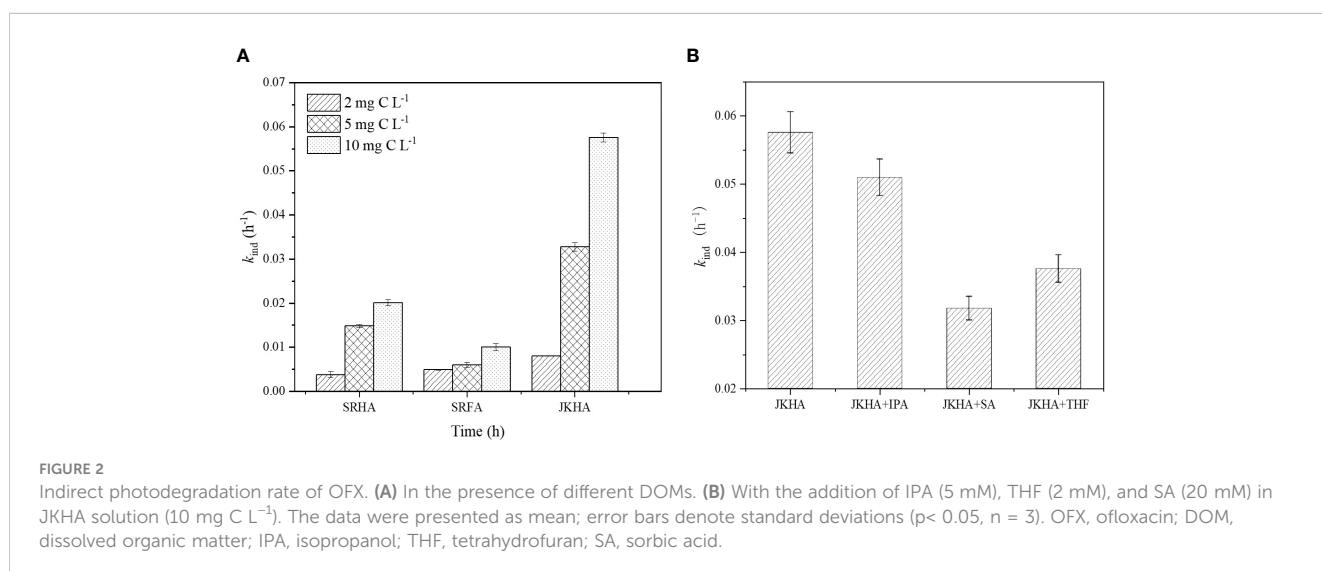
In this study, the indirect photodegradation of OFX was investigated in different DOM solutions. The proportion of indirect photodegradation in OFX photodegradation is calculated in Table S2. In contrast, the indirect photodegradation rate of OFX increased irregularly with the increasing concentration (Figure 2A). It may be due to DOM having a dual effect on the indirect photodegradation of OFX. DOM can promote the indirect photodegradation of OFX by producing more RIs with increasing DOM concentration (Bai et al., 2018). Additionally, DOM can also inhibit indirect photodegradation by scavenging or reducing RIs. The combination of the stimulatory and inhibitory effects led to an irregular change in the rate of indirect photodegradation of OFX.

3.2.2 Roles of reactive intermediates

Many studies proved that indirect photodegradation was mediated by RIs derived from DOM. Wang et al. (2018) reported that three sulfonamide antibiotics were degraded by $^3DOM^*$ -induced indirect photodegradation. $\cdot OH$ -mediated oxidation made more contributions to the indirect photodegradation of atrazine and S-metolachlor (Drouin et al., 2021). To further probe the effect of RIs on the indirect photodegradation of OFX, different scavengers were added to the OFX solutions containing JKHA. IPA was used as a scavenger to eliminate $\cdot OH$ (Ye et al., 2022), and the roles of $^3DOM^*$ and 1O_2 were explored by the addition of SA and THF, respectively (Mateus et al., 2000; Han et al., 2017). As can be seen from Figure 2B, IPA did not significantly inhibit the indirect photodegradation of OFX compared to other scavengers, suggesting that the effect of $\cdot OH$ was minor on the indirect photodegradation of OFX. In contrast, the indirect photodegradation rate was significantly reduced with the addition of SA and THF, indicating that $^3DOM^*$ and 1O_2 might dominate OFX indirect photodegradation. According to the indirect photodegradation rates of OFX with the addition of different quenchers, the contribution of RIs is shown in Table S3.

3.2.3 Roles of DOM fluorescent components

There were prominent different structural and compositional variability among DOM from different sources. Compared with DOM extracted from seawater, DOM from mariculture areas contained higher humic-like substances and aromatic and carbonyl structures, which exhibited a higher concentration of $^3DOM^*$ to promote the photodegradation of sulfonamide (Wang et al., 2018). Therefore, EEMs-PARAFAC analysis was used to divide DOM into four different fluorescent components to investigate the roles of DOM components in OFX indirect photodegradation (Figure 3; Table S4). The maximum Ex/Em peak of component 1 (C1) was 420/500 nm. The spectra of C1 were the same as those reported in earlier studies (Yamashita et al., 2015). This component can be characterized as aromatic and high-



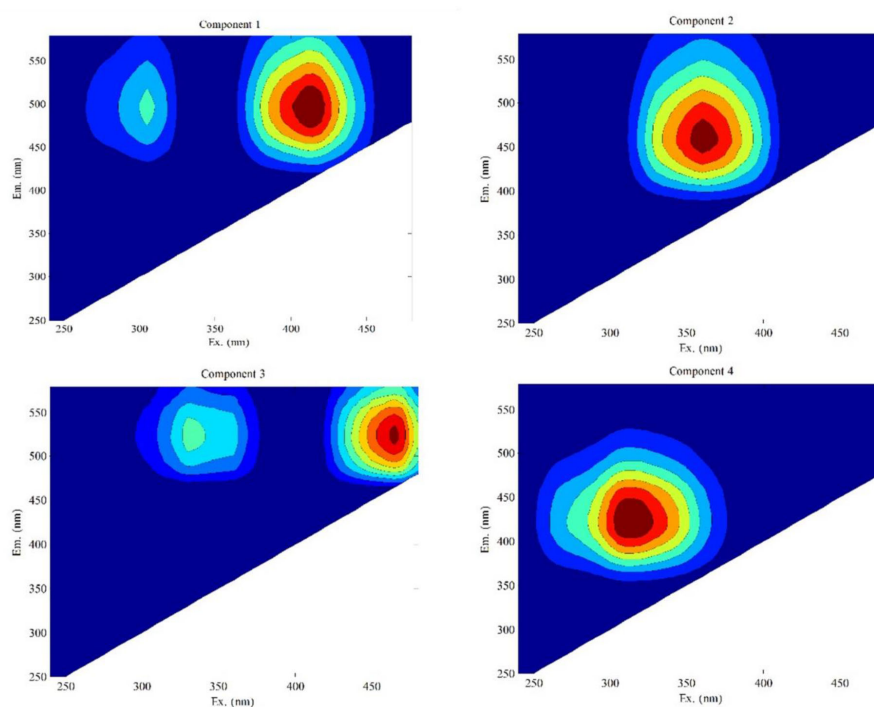


FIGURE 3

Fluorescence signatures of the four identified EEMs-PARAFAC components. EEMs-PARAFAC, fluorescence excitation–emission matrix spectroscopy–parallel factor analysis.

molecular-weight terrestrial humic-like materials (Kowalczyk et al., 2010). Component 2 (C2) exhibited broad excitation and emission maxima at 370 and 460 nm, which were typically observed as humic-like in the terrestrial environment (Quang et al., 2016). Component 3 (C3) had a maximum fluorescence peak at Ex/Em = 460/520 nm. The fluorescence peak position of C3 was similar to the reported soil fulvic acid known as the previous commercially available “Contech” FA (emission maxima occur at 492–521 nm, corresponding to excitation at 350–455 nm) (Lochmueller and Saavedra, 1986). Component 4 (C4) showed the Ex/Em wavelength of the fluorescence peak at 320/440 nm. Coble et al. (1998) found a fluorescent component that had an excitation maximum of 320 nm and an emission maximum of 420 nm in the Arabian Sea. The peak was considered to be present in visible humic-like. DOM with higher molecular weight may contain higher aromaticity, and the EEM peak occurred as a red-shift as molecular weight increased (Wei et al., 2016). Therefore, the molecular weights of the four components might be $C3 > C1 > C2 > C4$. The maximum Ex/Em wavelengths of C3 might be due to increasing molecular weight and aromaticity (Baker and Inverarity, 2004). Additionally, we determined the fluorescence intensities of the four DOM components at 0 and 24 h, respectively (Table S5). It showed that the JKHA solution had the max total fluorescence intensity at the same DOC concentration, followed by SRFA and SRHA. After irradiation, the fluorescence intensity of C1, C2, and C3 decreased, else than C4. It may be because C4 cannot be excited effectively on account of the irradiation below 320 nm being the cutoff.

The proportion of indirect photodegradation in OFX photodegradation is calculated in Table S2. The indirect photodegradation of OFX accounted for 52.5%–95.4% of the JKHA solution. However, in SRFA and SRHA solutions, the indirect photodegradation of OFX only accounted for 35.6%–62.7% and 30.5%–80.1%, respectively. The results indicated that the indirect photodegradation was affected by the source and characteristics of DOM. To further research the mechanism of OFX indirect photodegradation in the presence of DOM solutions, we used PC to determine the steady-state concentrations of RIs in DOM solutions. The concentration of RIs increased with the DOM concentration (Table S6). Furthermore, the concentration of RIs in the JKHA solution was significantly higher than in other DOM solutions. It indicated that the JKHA solution can generate more RIs than other DOM solutions to promote the indirect photodegradation of OFX.

Additionally, Pearson’s correlation analysis was carried out to explore the relationship between the DOM fluorescence intensity and the concentration of RIs (Table 1). The four fluorescence components had significant correlations with the concentration of RIs, suggesting that the photolysis of the four DOM components can generate RIs. It might contribute to the indirect photodegradation of OFX. The ability of the four fluorescent components to produce RIs can be evaluated as $C1 > C3 > C4 > C2$. Meanwhile, C3 and C1 were the two main components in the JKHA solution (Table S5). Figure 2B pointed out that 1O_2 and $^3DOM^*$ were the main RIs to promote the indirect photodegradation of

OFX. Therefore, the indirect photodegradation of OFX may be the fastest in the JKHA solution because there were high contents of C1 and C3, which can produce more $^1\text{O}_2$ and $^3\text{DOM}^*$. The correlations among the OFX indirect photodegradation rate and four DOM components are shown in Table 1. The correlation order of the four DOM components was $\text{C1} > \text{C3} > \text{C2} > \text{C4}$, which indicated that C1 and C3 made more contributions than C2 and C4 to the indirect photodegradation of OFX. It confirmed that the large-molecular-weight DOM contributes the most to the indirect photodegradation of OFX.

HIX and SUVA_{254} were used to further explore the influence of DOM structure on OFX indirect photodegradation. SUVA_{254} was significantly correlated with the concentrations of $^1\text{O}_2$ and $^3\text{DOM}^*$ (Table 1), indicating that highly aromatic DOM can produce more RIs. The aromatic structure was the main chromophore of DOM, which can absorb solar radiation, produce $^1\text{DOM}^*$ in natural environmental water, and act on the formation of $^3\text{DOM}^*$ (Boyle et al., 2009). The correlation between the indirect photodegradation rate of OFX and HIX is shown in Table 1, which indicated that terrestrial DOM with high humification contributed more to the indirect photodegradation of OFX. In Figure 2A, the OFX indirect photodegradation rate in the JKHA solution was prominently higher than that in other DOM solutions. This may be due to the higher SUVA_{254} and HIX values of JKHA, which had a higher aromatic structure when compared to SRHA and SRFA. Therefore, higher concentrations of RIs can be generated in the JKHA solution to promote the indirect photodegradation of OFX.

Moreover, redundancy analysis (RDA) was conducted between DOM fluorescence components, HIX, and SUVA_{254} with RIs, k_{ind} . The RDA results revealed that the composition and properties of DOM can explain the variation in the database (96.53%) (Figure S2). HIX, SUVA_{254} , $^3\text{DOM}^*$, and $^1\text{O}_2$ were positively correlated with the indirect photodegradation rate of OFX. The finding was in accordance with the results of Pearson's correlation analysis.

3.3 Effects of environmental factors on the OFX indirect photodegradation

3.3.1 Effect of salinity

Environmental factors in seawater were important factors affecting the indirect photodegradation of organic contaminants. Trovo et al. (2009) studied the photodegradation phenomenon in freshwater and seawater, discovering that the photodegradation rate of sulfamethoxazole decreased after 7 h in simulated seawater. Sirtori et al. (2010) found that trimethoprim had a faster photodegradation rate in freshwater while showing a longer photodegradation time in seawater. de Bruyn et al. (2012) reported that it made no difference in the photodegradation rate of phenanthrene in seawater and freshwater. In contrast, the photodegradation rate of acetaminophen increased with the increase in salinity (Bai et al., 2018). In this study, the indirect photodegradation of OFX at different salinities in the JKHA solution was explored. Figure 4A shows that when the salinity increased to 35‰, the OFX indirect photodegradation rate was significantly enhanced, and the indirect photodegradation rate at $S = 35\text{‰}$ was approximately two times that at $S = 5\text{‰}$. Previous studies pointed out that the photodegradation of organic pollutants was affected by ionic strength, metal ions, and halogen ions in seawater (Zhao et al., 2019). Firstly, Fe^{2+} was contained in seawater, and Fe^{2+} can react with H_2O_2 to convert many organic compounds into inorganic compounds, which can effectively remove some refractory contaminants. Secondly, higher ionic strength can also reduce the attenuation rate of $^3\text{DOM}^*$, resulting in the promotion of the indirect photodegradation of OFX initiated by $^3\text{DOM}^*$, $\cdot\text{OH}$, and $^1\text{O}_2$ (Zhang et al., 2019). Thirdly, some halogen ions can produce halogen active radicals to react with electron-rich chromophores to accelerate the removal of antibiotics (Eqs 18, 19) (Lin et al., 2013). Finally, high salinity can increase the number of photolysis electrons in the hydrated DOM, thus increasing the

TABLE 1 Correlations among the OFX indirect photodegradation rate, DOM components, HIX, SUVA_{254} , and the steady-state concentrations of RIs.

	C1	C2	C3	C4	HIX	$^1\text{O}_2$	$\cdot\text{OH}$	$^3\text{DOM}^*$	k_{ind}	SUVA_{254}
C1	1	.902**	.992**	.943**	.990**	.983**	.816**	.996**	.938**	.896**
C2		1	.843**	.976**	.919**	.830**	.858**	.887**	.824*	.749*
C3			1	.900**	.977**	.990**	.776*	.990**	.937**	.902**
C4				1	.935**	.900**	.773*	.935**	.815*	.798**
HIX					1	.952**	.862**	.977**	.964**	.847**
$^1\text{O}_2$						1	.737*	.993**	.917**	.916**
$\cdot\text{OH}$							1	.798*	.905**	.752*
$^3\text{DOM}^*$								1	.936**	.909**
k_{ind}									1	.777*
SUVA_{254}										1

OFX, ofloxacin; DOM, dissolved organic matter; HIX, humification index; RIs, reactive intermediates.

** Correlation is significant at the 0.01 level (two-tailed).

* Correlation is significant at the 0.05 level (two-tailed).

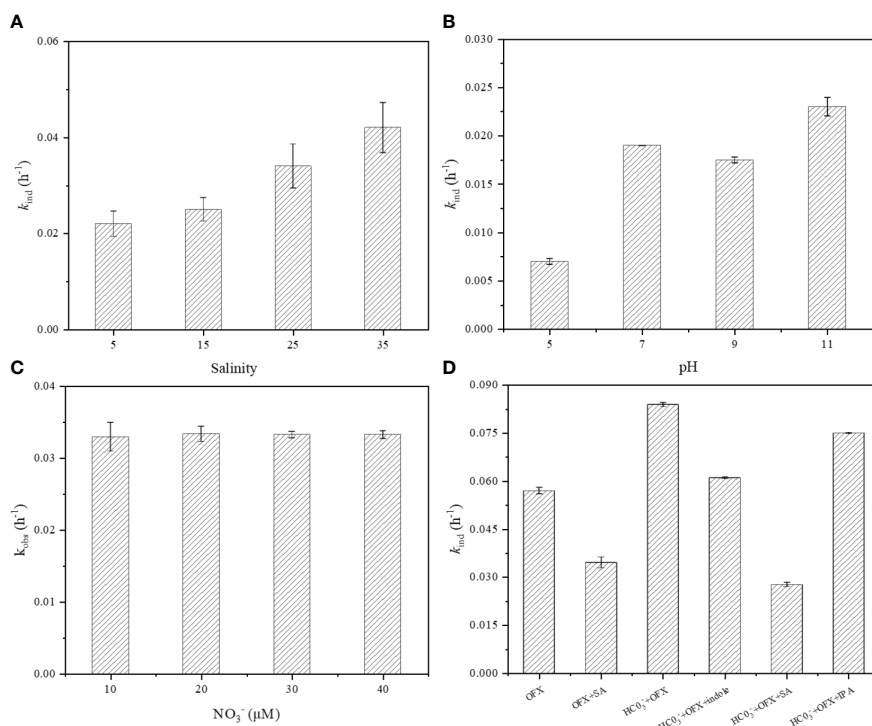


FIGURE 4

The indirect photodegradation rate of OFX at different (A) salinity and (B) pH values, (C) NO_3^- concentrations, and (D) radical quenchers (indole = 200 μM , HCO_3^- = 2 mM, IPA = 100 mM, and SA = 2 mM). All solutions were prepared with JKHA (10 mg C L⁻¹). The data were presented as mean; error bars denote standard deviations ($p < 0.05$, $n = 3$). OFX, ofloxacin; IPA, isopropanol; SA, sorbic acid.

rate of $\cdot OH$ formation by increasing the content of H_2O_2 to improve the indirect photodegradation of OFX (Anastasio and Newberg, 2007).



3.3.2 Effect of pH

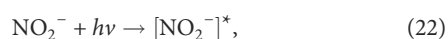
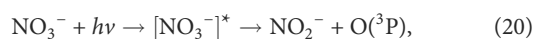
pH can affect the formation of RIs and the structure of pollutants to influence the photodegradation of organic pollutants. Previous studies found that the degradation of OFX by bimetallic doped catalysts exhibited high pH dependence (Tian et al., 2021), while the indirect photodegradation of OFX at different pH in simulated seawater was rarely studied. To explore the influence of pH on the indirect photodegradation of OFX in simulated seawater, we determined the indirect photodegradation rate of OFX from pH 5.0 to 11.0 in the JKHA solution. The indirect photodegradation rate of OFX was complex at different pH values (Figure 4B). When the pH increased to 7.0, the indirect photodegradation rate was nearly three times that at pH 5.0. The pK_{a1} and pK_{a2} values of OFX have been reported to be 6.1 and 8.3, respectively (Luo et al., 2019). The existing forms of OFX changed from cation to zwitterion when pH was from 5.0 to 7.0. Fluoroquinolone makes it difficult for the defluorination process to occur under acidic conditions (Albini and Monti, 2003). Moreover, the main ionizable groups of OFX were the piperazine ring and the carboxyl. The electron cloud density was relatively high in the

presence of zwitterion, and the piperazine ring of OFX was susceptible to electrophilic attack, resulting in a higher indirect photodegradation rate. However, when pH was in the range of 7.0 to 9.0, the decrease in electron cloud density led to a decrease in electrophilic attack, resulting in a decrease in the indirect photodegradation rate (Zhu et al., 2020). The indirect photodegradation rate increased continually at pH 11.0, and it was likely due to the high pH enhancing the role of 1O_2 and $\cdot OH$ and facilitating the indirect photodegradation of OFX (Bai et al., 2018).

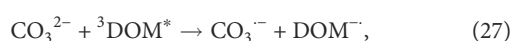
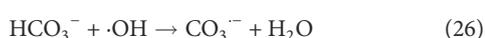
3.3.3 Effects of nitrate and bicarbonate

Many studies have demonstrated that nitrate can produce $\cdot OH$ to facilitate the photodegradation of organic pollutants in natural water (Zepp et al., 1987; Warneck and Wurzinger, 1988). The concentration of nitrate was approximately from 10^{-5} to 10^{-3} M in natural water, which was affected by the geographical environment and human activities. In this study, nitrate-induced indirect photodegradation of OFX was explored in a solution containing JKHA under simulated irradiation. The indirect photodegradation rate fluctuated by approximately $0.033 h^{-1}$ with the increase in the concentration of nitrate (Figure 4C). It demonstrated that increased nitrate concentration had little effect on the indirect photodegradation of OFX. Other studies also discovered the same phenomenon of sulfadiazine and sulfamerazine (Bai et al., 2021; Tang et al., 2021). John Mack (1999) reported that the direct photolysis of nitrate was related to the formation of $\cdot OH$ and nitrite, but nitrite was always considered

an excellent scavenger for $\cdot\text{OH}$. The sunlight absorption rate constant of nitrate increased sharply at 300–320 nm (Zepp et al., 1987), and the formation rate of $\cdot\text{OH}$ was 9.1% during irradiation at approximately 320 nm at pH 8.0 (Warneck and Wurzinger, 1988). However, we used a filter to remove irradiation below 320 nm, which limited the production of $\cdot\text{OH}$. Meanwhile, $\cdot\text{OH}$ contributed less to the indirect photodegradation of OFX according to the quenching experiments described in Section 3.3. Thus, the indirect photodegradation rate of OFX was not affected by the increasing nitrate concentration.



Bicarbonate was the ubiquitous inorganic salt present in natural water, which can produce CO_3^{2-} to promote the photodegradation of organic contaminants (Eqs 25–28) (Yan et al., 2019). It is well known that $\cdot\text{OH}$ can react very rapidly with almost any organic compound, but CO_3^{2-} has high selectivity, and its concentration in the surface water exposed to sunlight was approximately hundreds of times higher than that of $\cdot\text{OH}$ (Canonica et al., 2005). The role of CO_3^{2-} may thus be important in controlling the persistence of various organic contaminants. It found that the indirect photodegradation rate of OFX increased significantly at pH 8.0 after the addition of HCO_3^- (Figure 4D). In this study, indole, IPA, and SA were added to the HCO_3^- solution containing JKHA to explore the formation of RIs ($S = 30\%$, $\text{pH} = 8.0$). After the addition of indole, the OFX indirect photodegradation rate was close to that without HCO_3^- addition. It suggested that CO_3^{2-} was the main factor promoting the OFX indirect photodegradation. Then, experiments were performed in the presence of SA and IPA in the HCO_3^- solution to explore the generation mechanism of CO_3^{2-} . The indirect photodegradation rate decreased significantly after adding SA but was lower than that of $k_{\text{ind,OFX+SA}}$ (Figure 4D), indicating that the ${}^3\text{DOM}^*$ was responsible for the formation of CO_3^{2-} . After the addition of IPA, the indirect photodegradation rate of OFX was decreased, suggesting that $\cdot\text{OH}$ was responsible for the formation of HCO_3^- .



4 Conclusion

In this study, we investigated the effects of DOM and environmental factors on OFX indirect photodegradation. DOM was believed to enhance the indirect photodegradation of OFX due to the generation of RIs. Quenching experiments confirmed the roles of ${}^1\text{O}_2$ and ${}^3\text{DOM}^*$ in the indirect photodegradation of OFX in the JKHA solution. DOM was divided into four components by using EEMs-PARAFAC, and terrestrial humic-like components made more contributions to the indirect photodegradation of OFX by producing more RIs. The difference between indirect photodegradation of OFX in different DOM solutions was due to the structure of DOM. The indirect photodegradation of OFX was enhanced with salinity, which may be related to the halogen active radicals and the production of RIs. The indirect photodegradation of OFX by pH was complex because pH can affect both the structure of OFX and the production of RIs. NO_3^- had no significant effect on the indirect photodegradation of OFX, while HCO_3^- promoted the indirect photodegradation of OFX, and CO_3^{2-} may be the main RIs responsible for OFX indirect photodegradation in HCO_3^- solution. This study was important for assessing the ecological risk and environmental fate of OFX.

Data availability statement

The original contributions presented in the study are included in the article/Supplementary Material. Further inquiries can be directed to the corresponding authors.

Author contributions

SL: conceptualization, methodology, formal analysis, data analysis, and writing of the original draft. ZC: project administration and funding acquisition. YB: project administration, funding acquisition, and writing—review and editing. DD: investigation and visualization. JY: conceptualization and methodology. RS: project administration and writing—review and editing. KQ: project administration and funding acquisition. All authors contributed to the article and approved the submitted version.

Funding

This work was supported by the National Natural Science Foundation of China (grant number 41906129), the Natural Science Foundation of Shandong Province, China (grant number ZR2019BD004), the National Natural Science Foundation of China-Shandong Province Joint Fund (grant number U1806214) and the Basic Research Foundation of Chinese Academy of Fishery Sciences (grant number 2020TD49).

Conflict of interest

The authors declare that the research was conducted in the absence of any commercial or financial relationships that could be construed as a potential conflict of interest.

Publisher's note

All claims expressed in this article are solely those of the authors and do not necessarily represent those of their affiliated

organizations, or those of the publisher, the editors and the reviewers. Any product that may be evaluated in this article, or claim that may be made by its manufacturer, is not guaranteed or endorsed by the publisher.

Supplementary material

The Supplementary Material for this article can be found online at: <https://www.frontiersin.org/articles/10.3389/fmars.2023.1132216/full#supplementary-material>

References

- Al Aukidy, M., Verlicchi, P., Jelic, A., Petrovic, M., and Barcelo, D. (2012). Monitoring release of pharmaceutical compounds: occurrence and environmental risk assessment of two WWTP effluents and their receiving bodies in the po valley, Italy. *Sci. Total Environ.* 438, 15–25. doi: 10.1016/j.scitotenv.2012.08.061
- Albini, A., and Monti, S. (2003). Photophysics and photochemistry of fluoroquinolones. *Chem. Soc. Rev.* 32, 238–250. doi: 10.1039/b209220b
- Anastasio, C., and Newberg, J. T. (2007). Sources and sinks of hydroxyl radical in sea-salt particles. *J. Geophys. Res. Atmos.* 112, D10. doi: 10.1029/2006JD008061
- Bai, Y., Cui, Z., Su, R., and Qu, K. J. C. (2018). Influence of DOM components, salinity, pH, nitrate, and bicarbonate on the indirect photodegradation of acetaminophen in simulated coastal waters. *Chemosphere* 205, 108–117. doi: 10.1016/j.chemosphere.2018.04.087
- Bai, Y., Zhou, Y., Che, X., Li, C., Cui, Z., Su, R., et al. (2021). Indirect photodegradation of sulfadiazine in the presence of DOM: Effects of DOM components and main seawater constituents. *Environ. pollut.* 268, 115689. doi: 10.1016/j.envpol.2020.115689
- Baker, A., and Inverarity, R. (2004). Protein-like fluorescence intensity as a possible tool for determining river water quality. *Hydrol. Process.* 18, 2927–2945. doi: 10.1002/hyp.5597
- Bodrato, M., and Vione, D. (2014). APEX (Aqueous photochemistry of environmentally occurring xenobiotics): a free software tool to predict the kinetics of photochemical processes in surface waters. *Environ. Sci. Process. Impacts.* 16, 732–740. doi: 10.1039/c3em00541k
- Boyle, E. S., Guerriero, N., Thiallet, A., Vecchio, R. D., and Blough, N. V. (2009). Optical properties of humic substances and CDOM: relation to structure. *Environ. Sci. Technol.* 43, 2262–2268. doi: 10.1021/es803264g
- Burns, J. M., Cooper, W. J., Ferry, J. L., King, D. W., DiMento, B. P., McNeill, K., et al. (2012). Methods for reactive oxygen species (ROS) detection in aqueous environments. *Aquat. Sci.* 74, 683–734. doi: 10.1039/d1em00246e
- Canonica, S., Kohn, T., Mac, M., Real, F. J., Wirz, J., and von Gunten, U. (2005). Photosensitizer method to determine rate constants for the reaction of carbonate radical with organic compounds. *Environ. Sci. Technol.* 39, 9182–9188. doi: 10.1039/d1em00246e
- Cheng, D., Liu, H., Yang, E., Liu, F., Lin, H., and Liu, X. (2021). Effects of natural colloidal particles derived from a shallow lake on the photodegradation of ofloxacin and ciprofloxacin. *Sci. Total Environ.* 773, 145102. doi: 10.1016/j.scitotenv.2021.145102
- Coble, P. G., Del Castillo, C. E., and Avril, B. (1998). Distribution and optical properties of CDOM in the Arabian Sea during the 1995 southwest monsoon. *Deep Sea Res. Part II* 45, 2195–2223. doi: 10.1016/S0967-0645(98)00068-X
- Danner, M. C., Robertson, A., Behrends, V., and Reiss, J. (2019). Antibiotic pollution in surface fresh waters: Occurrence and effects. *Sci. Total Environ.* 664, 793–804. doi: 10.1016/j.scitotenv.2019.01.406
- de Bruyn, W. J., Clark, C. D., Ottelle, K., and Aiona, P. (2012). Photochemical degradation of phenanthrene as a function of natural water variables modeling freshwater to marine environments. *Mar. pollut. Bull.* 64, 532–538. doi: 10.1016/j.marpolbul.2011.12.024
- Ding, G., Chen, G., Liu, Y., Li, M., and Liu, X. (2020). Occurrence and risk assessment of fluoroquinolone antibiotics in reclaimed water and receiving groundwater with different replenishment pathways. *Sci. Total Environ.* 738, 139802. doi: 10.1016/j.scitotenv.2020.139802
- Drouin, G., Droz, B., Leresche, F., Payraudeau, S., Masbou, J., and Imfeld, G. (2021). Direct and indirect photodegradation of atrazine and s-metolachlor in agriculturally impacted surface water and associated c and n isotope fractionation. *Environ. Sci.: Process. Impacts.* 23, 1791–1802. doi: 10.1039/d1em00246e
- Du, Y., Chen, H., Zhang, Y., and Chang, Y. (2014). Photodegradation of gallic acid under UV irradiation: insights regarding the pH effect on direct photolysis and the ROS oxidation-sensitized process of DOM. *Chemosphere* 99, 254–260. doi: 10.1016/j.chemosphere.2013.10.093
- Fu, J., Mai, B., Sheng, G., Zhang, G., Wang, X., Xiao, X., et al. (2003). Persistent organic pollutants in environment of the pearl river delta, China: an overview. *Chemosphere* 52, 1411–1422. doi: 10.1016/s0045-6535
- Ge, L., Chen, J., Wei, X., Zhang, S., Qiao, X., Cai, X., et al. (2010). Aquatic photochemistry of fluoroquinolone antibiotics: kinetics, pathways, and multivariate effects of main water constituents. *Environ. Sci. Technol.* 44, 2400–2405. doi: 10.1021/es902852v
- Guéguen, C., Granskog, M. A., McCullough, G., and Barber, D. G. (2011). Characterisation of colored dissolved organic matter in Hudson bay and Hudson strait using parallel factor analysis. *J. Maine Syst.* 88, 423–433. doi: 10.1016/j.jmarsys.2010.12.001
- Guerard, J. J., Miller, P. L., Trouts, T. D., and Chin, Y.-P. (2009). The role of fulvic acid composition in the photosensitized degradation of aquatic contaminants. *Aquat. Sci.* 71, 160–169. doi: 10.1007/s00027-009-9192-4
- Han, X., Li, Y., Li, D., and Liu, C. (2017). Role of free Radicals/Reactive oxygen species in MeHg photodegradation: Importance of utilizing appropriate scavengers. *Environ. Sci. Technol.* 51, 3784–3793. doi: 10.1021/acs.est.7b00205
- Kowalczyk, P., Cooper, W. J., Durako, M. J., Kahn, A. E., Gonsior, M., and Young, H. (2010). Characterization of dissolved organic matter fluorescence in the south Atlantic bight with use of PARAFAC model: Relationships between fluorescence and its components, absorption coefficients and organic carbon concentrations. *Mar. Chem.* 118, 22–36. doi: 10.1016/j.marchem.2009.10.002
- Lam, M. W., and Mabury, S. A. (2005). Photodegradation of the pharmaceuticals atorvastatin, carbamazepine, levofloxacin, and sulfamethoxazole in natural waters. *Aquat. Sci.* 67, 177–188. doi: 10.1007/s00027-004-0768-8
- Lin, A. Y., Wang, X. H., and Lee, W. N. (2013). Phototransformation determines the fate of 5-fluorouracil and cyclophosphamide in natural surface waters. *Environ. Sci. Technol.* 47, 4104–4112. doi: 10.1021/es304976q
- Liu, H., Pu, Y., Qiu, X., Li, Z., Sun, B., Zhu, X., et al. (2021). Humic acid extracts leading to the photochemical bromination of phenol in aqueous bromide solutions: Influences of aromatic components, polarity and photochemical activity. *Molecules* 26(3), 608. doi: 10.3390/molecules26030608
- Liu, T., Yin, K., Liu, C., Luo, J., Crittenden, J., Zhang, W., et al. (2018). The role of reactive oxygen species and carbonate radical in oxcabazepine degradation via UV, UV/H₂O₂: Kinetics, mechanisms and toxicity evaluation. *Water Res.* 147, 204–213. doi: 10.1016/j.watres.2018.10.007
- Lochmueller, C. H., and Saavedra, S. S. (1986). Conformational changes in a soil fulvic acid measured by time-dependent fluorescence depolarization. *Anal. Chem.* 58, 1978–1981. doi: 10.1021/ac00122a014
- Luo, X., Wei, X., Chen, J., Xie, Q., Yang, X., and Peijnenburg, W. (2019). Rate constants of hydroxyl radicals reaction with different dissociation species of fluoroquinolones and sulfonamides: Combined experimental and QSAR studies. *Water Res.* 166, 115083. doi: 10.1016/j.watres.2019.115083
- Mack, J., and Bolton, J. R. 1999. Photochemistry of nitrite and nitrate in aqueous solution: a review[J]. *Journal of Photochemistry and Photobiology A: Chemistry*, 128(1–3), 1–3. doi: 10.1016/s1010-6030(99)00155-0
- Mateus, M. C. D., Da Silva, A. M., and Burrows, H. D. (2000). Kinetics of photodegradation of the fungicide fenarimol in natural waters and in various salt solutions: salinity effects and mechanistic considerations. *Water Res.* 34, 1119–1126. doi: 10.1016/S0043-1354(99)00254-7

- Niu, X.-Z., Busetti, F., Langsa, M., and Croué, J.-P. (2016). Roles of singlet oxygen and dissolved organic matter in self-sensitized photo-oxidation of antibiotic norfloxacin under sunlight irradiation. *Water Res.* 106, 214–222. doi: 10.1016/j.watres.2016.10.002
- Ohno and Technology (2002). Fluorescence inner-filtering correction for determining the humification index of dissolved organic matter. *Environ. Sci. Technol.* 36, 742–746. doi: 10.1021/es0155276
- Quang, V. L., Kim, H. C., Maqbool, T., and Hur, J. (2016). Fate and fouling characteristics of fluorescent dissolved organic matter in ultrafiltration of terrestrial humic substances. *Chemosphere* 165, 126–133. doi: 10.1016/j.chemosphere.2016.09.029
- Sirtori, C., Aguera, A., Gernjak, W., and Malato, S. (2010). Effect of water-matrix composition on trimethoprim solar photodegradation kinetics and pathways. *Water Res.* 44, 2735–2744. doi: 10.1016/j.watres.2010.02.006
- Tang, X., Cui, Z., Bai, Y., and Su, R. (2021). Indirect photodegradation of sulfathiazole mechanisms over FeCu doped g-C₃N₄ for ofloxacin degradation via the efficient peroxymonosulfate activation. *J. Clean. Prod.* 315, 128207. doi: 10.1016/j.jclepro.2021.128207
- Tian, Y., Li, Q., Zhang, M., Nie, Y., Tian, X., Yang, C., et al. (2021). pH-dependent oxidation mechanisms over FeCu doped g-C₃N₄ for ofloxacin degradation via the efficient peroxymonosulfate activation. *J. Clean. Prod.* 315, 128207. doi: 10.1016/j.jclepro.2021.128207
- Timko, S. A., Romera-Castillo, C., Jaffe, R., and Cooper, W. J. (2014). Photo-reactivity of natural dissolved organic matter from fresh to marine waters in the Florida Everglades, USA. *Environ. Sci. Process. Impacts.* 16, 866–878. doi: 10.1039/c3em00591g
- Trovo, A. G., Nogueira, R. F., Aguera, A., Sirtori, C., and Fernandez-Alba, A. R. (2009). Photodegradation of sulfamethoxazole in various aqueous media: persistence, toxicity and photoproducts assessment. *Chemosphere* 77, 1292–1298. doi: 10.1016/j.chemosphere.2009.09.065
- Wang, J., Chen, J., Qiao, X., Wang, Y., Cai, X., Zhou, C., et al. (2018). DOM from mariculture ponds exhibits higher reactivity on photodegradation of sulfonamide antibiotics than from offshore seawaters. *Water Res.* 144, 365–372. doi: 10.1016/j.watres.2018.07.043
- Wang, J., Chen, J., Qiao, X., Zhang, Y. N., Uddin, M., and Guo, Z. (2019). Disparate effects of DOM extracted from coastal seawaters and freshwaters on photodegradation of 2,4-dihydroxybenzophenone. *Water Res.* 151, 280–287. doi: 10.1016/j.watres.2018.12.045
- Wang, J., Wang, K., Zhang, L., Guo, Y., Guo, Z., Sun, W., et al. (2021). Mechanism of bicarbonate enhancing the photodegradation of beta-blockers in natural waters. *Water Res.* 197, 117078. doi: 10.1016/j.watres.2021.117078
- Warneck, P., and Wurzing, C. (1988). Product quantum yields for the 305-nm photodecomposition of nitrate in aqueous solution. *J. Phys. Chem. C.* 92, 6278–6283. doi: 10.1021/j100333a022
- Wei, Z., Wang, X., Zhao, X., Xi, B., Wei, Y., Zhang, X., et al. (2016). Fluorescence characteristics of molecular weight fractions of dissolved organic matter derived from composts. *Int. Biodeterior. Biodegrad.* 113, 187–194. doi: 10.1016/j.ibiod.2016.03.010
- Weishaar, J. L., Aiken, G. R., Bergamaschi, B. A., Fram, M. S., Fujii, R., and Mopper, K. J. (2003). Evaluation of specific ultraviolet absorbance as an indicator of the chemical composition and reactivity of dissolved organic carbon. *Environ. Sci. Technol.* 37, 4702–4708. doi: 10.1021/es030360x
- Wu, B., Arnold, W. A., and Ma, L. (2021). Photolysis of atrazine: Role of triplet dissolved organic matter and limitations of sensitizers and quenchers. *Water Res.* 190, 116659. doi: 10.1016/j.watres.2020.116659
- Xu, H., Guan, D.-X., Zou, L., Lin, H., and Guo, L. (2018). Contrasting effects of photochemical and microbial degradation on Cu (II) binding with fluorescent DOM from different origins. *Environ. Pollut.* 239, 205–214. doi: 10.1016/j.envpol.2018.03.108
- Yamashita, Y., McCallister, S. L., Koch, B. P., Gonsior, M., and Jaffé, R. (2015). Dynamics of dissolved organic matter in fjord ecosystems: Contributions of terrestrial dissolved organic matter in the deep layer. *Estuarine Coast. Shelf Sci.* 159, 37–49. doi: 10.1016/j.ecss.2015.03.024
- Yan, S., Liu, Y., Lian, L., Li, R., Ma, J., Zhou, H., et al. (2019). Photochemical formation of carbonate radical and its reaction with dissolved organic matters. *Water Res.* 161, 288–296. doi: 10.1016/j.watres.2019.06.002
- Yang, W., Abdelmelek, S. B., Zheng, Z., An, T., Zhang, D., Son, W., et al. (2013). Photochemical transformation of terbutaline (pharmaceutical) in simulated natural waters: Degradation kinetics and mechanisms. *J. Water Res.* 47 (17), 6558–6565. doi: 10.1016/j.watres.2013.08.029
- Yang, Y., Ok, Y. S., Kim, K. H., Kwon, E. E., and Tsang, Y. F. (2017). Occurrences and removal of pharmaceuticals and personal care products (PPCPs) in drinking water and water/sewage treatment plants: A review. *Sci. Total Environ.* 596–597, 303–320. doi: 10.1016/j.scitotenv.2017.04.102
- Ye, Z., Guo, Z., Wang, J., Zhang, L., Guo, Y., Yoshimura, C., et al. (2022). Photodegradation of acebutolol in natural waters: Important roles of carbonate radical and hydroxyl radical. *Chemosphere* 287, 132318. doi: 10.1016/j.chemosphere.2021.132318
- Zepp, R. G., Hoigne, J., and Bader, H. (1987). Nitrate-induced photooxidation of trace organic chemicals in water. *Environ. Sci. Technol.* 21, 443–450. doi: 10.1021/es00159a004
- Zhang, S. Q., Li, P., Zhao, X. L., He, S. W., Xing, S. Y., Cao, Z. H., et al. (2021). Hepatotoxicity in carp (*Cyprinus carpio*) exposed to environmental levels of norfloxacin (NOR): Some latest evidences from transcriptomics analysis, biochemical parameters and histopathological changes. *Chemosphere* 283, 131210. doi: 10.1016/j.chemosphere.2021.131210
- Zhang, R., Tang, J., Li, J., Zheng, Q., Liu, D., Chen, Y., et al. (2013). Antibiotics in the offshore waters of the bohai Sea and the yellow Sea in China: occurrence, distribution and ecological risks. *Environ. pollut.* 174, 71–77. doi: 10.1016/j.envpol.2012.11.008
- Zhang, Y. N., Zhao, J., Zhou, Y., Qu, J., Chen, J., Li, C., et al. (2019). Combined effects of dissolved organic matter, pH, ionic strength and halides on photodegradation of oxytetracycline in simulated estuarine waters. *Environ. Sci. Process. Impacts.* 21, 155–162. doi: 10.1039/c8em00473k
- Zhao, Q., Fang, Q., Liu, H., Li, Y., Cui, H., Zhang, B., et al. (2019). Halide-specific enhancement of photodegradation for sulfadiazine in estuarine waters: Roles of halogen radicals and main water constituents. *Water Res.* 160, 209–216. doi: 10.1016/j.watres.2019.05.061
- Zhu, X. D., Wang, Y. J., Liu, C., Qin, W. X., and Zhou, D. M. (2014). Kinetics, intermediates and acute toxicity of arsenic acid photolysis. *Chemosphere* 107, 274–281. doi: 10.1016/j.chemosphere.2013.12.060
- Zhu, Y., Wei, M., Pan, Z., Li, L., Liang, J., Yu, K., et al. (2020). Ultraviolet/peroxydisulfate degradation of ofloxacin in seawater: Kinetics, mechanism and toxicity of products. *Sci. Total Environ.* 705, 135960. doi: 10.1016/j.scitotenv.2019.135960